Doped β_{12}-borophene for CO_2 Reduction: A First Principles Investigation and Development of Generalising Software.

Samuel Jakes
Supervisors: Catherine Stampfl, Tanglaw Roman, and Oliver Conquest
SID: 470393815

(Dated: June 1, 2020)

The conversion of CO_2 into useful chemicals and fuels is a promising technology for simultaneously helping with the energy crisis and reducing the greenhouse gases in the atmosphere which contribute to climate change. One of the main obstacles for the realisation of economically viable CO_2 reduction is the lack of effective catalysts. Borophene, among other two-dimensional materials, has recently been shown to exhibit promising catalytic properties for this purpose. In this report, the effectiveness of Al-, Fe-, and Si-doped β_{12}-borophene is investigated, and software is presented that automates the process of investigating future catalysts.

INTRODUCTION

Climate change and the energy crisis are two of the greatest challenges facing modern society. Our dependence on fossil fuels as a source of energy has caused a massive increase in greenhouse gases. These gasses are causing widespread environmental damage and have the potential to cause far more in the near future [1]. The conversion of CO_2 into value added chemicals and fuels is a promising technology as a long term alternative to fossil fuels. Renewable energy sources could be used to power the conversion process, in which case the resulting chemicals provide a carbon neutral and essentially unlimited form of energy storage. This is particularly useful given that energy storage is currently the major bottleneck preventing renewable energies from competing with fossil fuels as mass energy sources [2]. Furthermore, developing the technology to efficiently remove CO_2 from the atmosphere may be important if efforts to extract greenhouses gases from the atmosphere are undertaken in the future.

Catalytic design for CO_2 reduction has proven to be difficult over the past few decades. CO_2 is a very energetically stable molecule, and so the reduction reaction requires high temperature and pressure. Effective catalysts must be stable under these conditions, highly selective, resistant to poisoning, made from affordable materials, and feasible to manufacture all while sufficiently lowering the CO_2 reduction reaction energy. Electrolysis provides an alternative method for the reduction of CO_2, generally requiring far milder reaction conditions. Recent studies of two-dimensional (2D) materials for electrocatalytic design have shown great promise due to their novel properties such as high specific surface area and high degree of flexibility. Borophene is one such 2D material, which when doped with transition metals shows many desirable catalyst properties for CO_2 reduction [3].

Density functional theory (DFT) is used in this report to explore the catalytic viability of Al-, Fe-, and Si-doped β_{12}-borophene for the conversion of CO_2 into value added chemicals. In particular, the conversion of CO_2 into CH_4 (methane) and CH_3OH (methanol), both of which are viable fuels, will be studied in this report. Of these two fuels, methanol is the preferred primary reduction product for several reasons. Firstly, methanol is a liquid at room temperature, while methane is a gas. As a consequence, methanol has a much higher energy density than methane (15.6 MJ/L vs 9.0 MJ/L [4]), even when methane is compressed under high pressure. Secondly, methane is an extremely potent greenhouse gas, with a global warming potential (GWP) of 84 over a twenty-year period [5]. This means that, averaged over twenty years, methane traps 84 times more heat than CO_2 per kg. As a result, if even minor leakages of methane occur during manufacture, distribution, and consumption, then the environmental damage will outweigh any benefit gained by storing renewable energy as a fuel. In contrast, methanol has no GWP because it's a liquid at room temperature.

The effectiveness of catalysts can be assessed based on their selectivity for methanol, and to some degree methane, as primary reaction products. It's also necessary for the catalysts to suppress the production of CO, which is a toxic gas that isn't very useful as a fuel. Fe-doped β_{12}-borophene has already been studied as a catalyst for CO_2 reduction using DFT by Liu et al, and was shown to be highly selective for methane [3]. Replicating this result here serves as a benchmark for the validity of the other results. Al- and Si-doped β_{12}-borophene are investigated here as CO_2 reduction catalysts for the first time. These elements are of particular interest because of their high earth abundance [6], which makes them reasonably

affordable. Additionally, Al and Si are rarely explored as potential catalysts, and so studying them here explores reasons for this. The catalytic performance of β_{12}-borophene with no dopant is also investigated, so that the effects of doping this material can be further investigated.
The lattice constants for β_{12}-borophene are determined, and shown to be in good agreement with other published values. The adsorption energies of Al-, Fe-, and Si-doped β_{12}-borophene are also calculated so that their energetic stability can be inferred. The reaction pathway energies for these catalysts are then automatically generated and plotted using software presented in this report. It is found that the results for Fe-doped β_{12}-borophene are in good agreement with those found in other research. The results also show that none of the newly investigated catalysts are suitable for CO_2 reduction.

DENSITY FUNCTIONAL THEORY

Density functional theory (DFT) is an important theoretical approach that has given rise to a state-of-the-art, computationally practical method for approximating ground-state solutions to the Schrödinger equation. The development of DFT was lead by Walter Kohn, which won him the Nobel Prize in Chemistry in 1998. The summary of DFT given here is based largely on the textbook "Density Functional Theory: A Practical Introduction" by David Sholl and Janice Steckel [7]. We begin by stating the time-dependent Schrödinger equation, which can be elegantly expressed in Dirac notation as:

$$i\hbar\frac{d}{dt}\left|\Psi\right\rangle = \hat{H}\left|\Psi\right\rangle,$$

where $\hat{H}$ is the Hamiltonian and Ψ is the total wave function of a given quantum system. The solutions to this equation are of great importance in studying the behaviour of materials on a quantum level because they describe how quantum systems will evolve in time given an initial set of parameters. In this sense, the Schrödinger equation can be thought of as a quantum analogue of Newton's second law, $F = ma$. However, unlike Newton's second law, solving the Schrödinger equation directly for the wave function is very difficult for many real-world systems. To illustrate this, we can examine one of the simplest methods of solving the wave function directly. This involves approximating the total wave function with the Hartree product, which is the product of individual electron wave functions. Since each electron wave function exists in 3 dimensional space, each wave function is a function of 3 spatial variables. Thus, the product of N electron wave functions is a function of 3N variables. For even remotely complicated systems the number of electrons, and hence variables, becomes far too large and computationally expensive to solve.
DFT provides a state-of-the-art method for circumventing these computational boundaries, effectively reducing the number of variables in our problem to a constant value of 3. There is, however, a caveat to this method - these solutions can only be found for the system's ground state. While limiting our solutions to the ground state is clearly a significant drawback, it turns out that a surprising number of useful physical properties can be deduced from only the ground-state solutions. A few pertinent examples include the bond lengths between molecules, the adsorption energies of molecules onto a surface, and preferred reaction pathways.
The goal of DFT is to find the ground-state energy of a given quantum system. The method for doing so is based on the first Kohn and Hohenberg theorem, which states that "the ground-state energy from Schrödinger's equation is a unique functional of the electron density" [7] (where a functional is simply a function of a function). This essentially says that the ground-state energy of a given quantum system can be determined from the system's ground-state electron density. Crucially, the theorem implies that there is a one-to-one mapping between the system's ground-state electron density and its ground-state energy.
The first Kohn and Hohenberg theorem is purely an existence theorem, so it doesn't tell us how to find the unique functional that converts ground-state electron density into ground-state energy. It also doesn't tell us which electron densities correspond to the desired solutions of the ground-state energy; it only says that there is a functional that provides a one-to-one mapping between these two properties. This is, naturally, where the second Kohn and Hohenberg theorem is useful. It states that "the electron density that minimizes the energy of the overall functional is the true electron density corresponding to the full solution of the Schrödinger equation." This means that if we can find a functional which maps ground-state electron density to ground-state energy, then our only remaining task is to vary the electron density until our functional is minimised. We will then have implicitly found the ground-state energy for our system, from which many properties of interest can be computed. While this is a remarkable theorem, its usefulness clearly rests upon our ability to find a functional that maps ground-state electron density to ground-state energy. Fortunately, the functional in question can be split into two simple components that make it possible to com-

pute:

$$E[\{\psi_i\}] = E_{known}[\{\psi_i\}] + E_{XC}[\{\psi_i\}],$$

where the known energy is a collection of terms for which the analytical solution can be computed (e.g. kinetic energies and Coulomb interactions), and the XC term is called the exchange correlation functional and includes everything else (e.g. quantum mechanical effects). Finding solutions for the E_{XC} term is a challenging problem in itself; however, great approximations have been found that show fantastic agreement with experiments. The most popular exchange correlation functionals come in two flavours: the local density approximation (LDA) [8] and the generalised gradient approximation (GGA) [9]. The former of these utilises the local electron density at every point in space, while the latter also takes into account the gradient of electron density. The exchange correlation approximation used in this report is the GGA [9], specifically the Perdew-Burke-Ernzerhof (PBE) exchange correlation functional [10].

One final problem needs to be addressed before the above method is useful: how can we find an electron density that we are sure minimises the functional for ground-state energy? For this we need the Kohn-Sham equations, which have the form:

$$[\frac{h^2}{2m}\nabla^2 + V(\mathbf{r}) + V_H(\mathbf{r}) + V_{XC}(\mathbf{r})]\psi_i(\mathbf{r}) = \epsilon_i\psi_i(\mathbf{r}),$$

where the ψ_i terms are the individual electron wave functions, and the V terms define potentials due to the electron-nuclei interactions, electron-electron interactions, and all other interactions, respectively. In defining these potentials, we have implicitly used the Born-Oppenheimer approximation. In this approximation, the positions of the electrons and atomic nuclei are treated separately because the electrons are much lighter than the atomic nuclei. As a consequence, the positions of the electrons are instantaneously adjusted to displacements of the atomic nuclei, while the converse is not true.

V_{XC} can be found for these equations from the derivative of E_{XC}:

$$V_{XC}(\mathbf{r}) = \frac{\delta E_{XC}(\mathbf{r})}{\delta n(\mathbf{r})}.$$

The solutions to the Kohn-Sham equations are single electron wave functions which only depend on 3 spatial dimensions, which is a property we desire for computational feasibility. Once the single electron wave functions have been found, the corresponding electron density can be found using

$$n(\mathbf{r}) = 2\sum_i \psi_i^*(\mathbf{r})\psi_i(\mathbf{r}),$$

where $n(\mathbf{r})$ is the electron density.

The process for finding the ground-state energy of the quantum system can now be summarised by an iterative process. An initial electron density is "guessed", from which the Kohn-Sham equation are solved to find the individual electron wave functions. These wave functions are then used to find a corresponding electron density. If this electron density is the same as (within a specified margin of error) the "guessed" electron density, then we know that this is the true electron density, which can be used to find the ground-state energy of the system. If the electron densities are significantly different, then we need to make further guesses until the electron densities are self-consistent. The details of this process, like many of the intricacies of DFT, are omitted here for the sake of brevity, but can be found in "Density Functional Theory: A Practical Introduction" [7].

COMPUTATIONAL METHODS

The Vienna Ab initio Simulation Package (VASP) [11–14] was used to perform the DFT calculations, employing a plane wave basis set. The exchange correlation functional used is the Generalised Gradient Approximation (GGA) [9], specifically the Perdew-Burke-Ernzerhof (PBE) pseudo-potentials [10]. Van der Waals forces were accounted for using DFT-D3 method with Becke-Johnson damping [15, 16]. In order to avoid interactions between separate borophene layers, a vacuum spacing of 15Å was used. For lattice constant determination, the energy difference convergence threshold was set to 10^{-6} eV, while for other calculations this was set to 10^{-4} eV. Monkhorst-Pack **k**-point grids were used for **k**-point sampling, with a size of $12 \times 20 \times 6$ for lattice constant determination of the unit cell and $3 \times 3 \times 2$ for other calculations which all used a 2×4 supercell. Initial magnetic moments were set for molecules and atoms to be 1.2 multiplied by their experimentally determined values, as recommended in the VASP documentation [17]. This lead to initial magnetic moments of 1.2 for Al, and 2.4 for both Fe and Si, and 0 for all other elements and molecules. For all calculations, the energy cutoff was set to 500 eV. Methfessel-Paxton smearing of order 1 was used for all calculations. The initial molecule configurations and bond lengths were determined in the Avagardo molecule editing platform [18] using the Universal Force Field (UFF) [19].

THEORETICAL METHODS

The concept of Gibbs free energy is useful for determining which reaction pathways are favourable. The change in Gibbs free energy at each reaction step is defined as

$$\Delta G = \Delta E + \Delta E_{ZPE} - T\Delta S + \Delta G_{pH}, \quad (1)$$

where ΔE is the reaction energy, ΔE_{ZPE} is the change in zero-point energy, T is the temperature of the system, ΔS is the change in entropy, and ΔG_{pH} is a change in energy due to contributions from the acidic solution in which the reaction takes place. Like many DFT calculations, the temperature is taken to be 0 K so that the entropy contributions can be ignored [20]. Similarly, the zero-point energy contribution can be considered insignificant for catalyst analysis, so it will also be ignored [21]. The contribution from the acidic solution is given by $\Delta G_{pH} = 2.303 k_B T \mathrm{pH}$, where in acidic solution we can set $\mathrm{pH} = 0$. These simplifications reduce the Gibbs free energy to

$$\Delta G = \Delta E. \quad (2)$$

This expression for Gibbs free energy will be assumed throughout this report.

The concept of adsorption energy is used to describe the strength of the interaction between dopants and the β_{12}-borophene surface. It can be defined mathematically as

$$E_{ads} = E_{S+D} - E_S - E_D, \quad (3)$$

where E_{ads} is the adsorption energy, E_{S+D} is the total energy of the dopant adsorbed on the β_{12}-borophene surface, E_S is the energy of the β_{12}-borophene surface, and E_D is the energy of the dopant. This can be physically interpreted as the energy gained by the process of adsorption, which is usually a negative value. Lower values (more negative) correspond to more exothermic interactions, which result in more energetically stable configurations. A similar equation exists for finding the ground-state energy of a particular reaction step:

$$E_{step} = E_{S+D+M} + E_{Spec}. \quad (4)$$

Where E_{step} is the ground-state energy of the reaction step, E_{S+D+M} is the ground-state energy of the intermediate molecule and the doped surface, and E_{Spec} is the ground-state energy of any spectator molecules involved in the reaction.

The potential determining step (PDS) is introduced to study the effectiveness of electrocatalysts. For electrocatalytic reactions, the PDS is often a simpler and more intuitive metric for determining the bottleneck of a reaction [22]. The PDS corresponds to the reaction step which has the greatest positive Gibbs free energy change along the reaction path with the lowest maximum Gibbs free energy change. To elaborate, finding the PDS first requires finding the reaction path between the reactants and products that has the lowest maximum increase in Gibbs free energy. The PDS is then the energy change of the step along this reaction pathway with the maximum change in Gibbs free energy.

Overpotentials are calculated from the PDS using the equation

$$\eta = U_{eq} + \frac{\Delta G_{PDS}}{ne}, \quad (5)$$

where η is the overpotential, U_{eq} is the equilibrium potential of the primary reduction product, ΔG_{PDS} is the change in Gibbs free energy at the PDS, n is the number of electrons transferred at the PDS and e is the elementary charge. The overpotential represents the minimum voltage needed to drive the electrolysis reaction.

A simplifying assumption about electrolysis is made throughout this report: the repeated protonation of CO_2 in acidic solution is modelled using diatomic hydrogen gas, so that the balanced net equation for the formation of methane is given by:

$$CO_2 + 4H_2 \longrightarrow CH_4 + 2H_2O \quad (6)$$

This is a standard simplifying assumption made in many first-principles electrochemical calculations [23]. Equation 6 is used to balance the intermediate reaction steps, so that the total numbers of C, O, and H atoms at each step are 1, 2, and 8, respectively. The balanced reaction steps are shown in Table I. Note that the formation of other products, such as CH_3OH and CO are also shown in this table. These balanced equations are used to plot the reaction pathway diagrams shown in this report. Since the relevant quantity for these diagrams is ΔG, the *change* in Gibbs free energy, it is convenient to centre the diagrams by subtracting the energy of the first reaction steps. This is done for every reaction pathway diagram in this report.

I. RESULTS AND DISCUSSION

The lattice constant was determined by varying the lattice constants a and b shown in the unit cell in Figure 1, while keeping the fractional coordinates of the molecules constant. The corresponding

R. State	Complete Formation Reaction
C*OOH	$CO_2+4H_2 \longrightarrow C^*OOH+3.5H_2$
O*CHO	$CO_2+4H_2 \longrightarrow O^*CHO+3.5H_2$
C*O	$C^*OOH+3.5H_2 \longrightarrow C^*O+H_2O+3H_2$
O*CHOH	$O^*CHO+3.5H_2 \longrightarrow O^*CHOH+3H_2$
C*OH	$C^*O+H_2O+3H_2 \longrightarrow C^*OH+H_2O+2.5H_2$
*+CO	$C^*O+H_2O+3H_2 \longrightarrow CO+H_2O+3H_2$
O*CH	$C^*O+H_2O+3H_2 \longrightarrow O^*CH+H_2O+2.5H_2$
C*HO	$O^*CHOH+3H_2 \longrightarrow C^*HO+H_2O+2.5H_2$
C*HOH	$C^*HO+H_2O+2.5H_2 \longrightarrow C^*HOH+H_2O+2H_2$
O^*CH_2	$C^*HO+H_2O+2.5H_2 \longrightarrow O^*CH_2+H_2O+2H_2$
C^*H+H_2O	$C^*HOH+H_2O+2H_2 \longrightarrow C^*H+2H_2O+1.5H_2$
C^*H_2OH	$C^*HOH+H_2O+2H_2 \longrightarrow C^*H_2OH+H_2O+1.5H_2$
O^*HCH_2	$O^*CH_2+H_2O+2H_2 \longrightarrow O^*HCH_2+H_2O+1.5H_2$
O^*CH_3	$O^*CH_2+H_2O+2H_2 \longrightarrow O^*CH_3+H_2O+1.5H_2$
CH_2	$C^*H_2OH+H_2O+1.5H_2 \longrightarrow CH_2+2H_2O+H_2$
HO^*CH_3	$O^*CH_3+H_2O+1.5H_2 \longrightarrow HO^*CH_3+H_2O+H_2$
O^*+CH_4	$O^*CH_3+H_2O+1.5H_2 \longrightarrow O^*+CH_4+H_2O+H_2$
$*+CH_3OH$	$HO^*CH_3+H_2O+H_2 \longrightarrow *+CH_3OH+H_2O+H_2$
C^*H_3	$CH_2+2H_2O+H_2 \longrightarrow CH_3+2H_2O+0.5H_2$
O^*H+CH_4	$O^*+CH_4+H_2O+H_2 \longrightarrow O^*H+CH_4+H_2O+0.5H_2$
“	$HO^*CH_3+H_2O+H_2 \longrightarrow O^*H+CH_4+H_2O+0.5H_2$
CH_4+H_2O	$O^*H+CH_4+H_2O+0.5H_2 \longrightarrow *+CH_4+2H_2O$
“	$CH_3+2H_2O+0.5H_2 \longrightarrow *+CH_4+2H_2O$

TABLE I. Reaction states (R. states) and their complete formation reactions, which include the spectator molecules. These equations are used for plotting the energies at each step in the reaction pathway diagrams. Note that a ditto (“) is used to indicate an alternative formation reaction for the above reaction state.

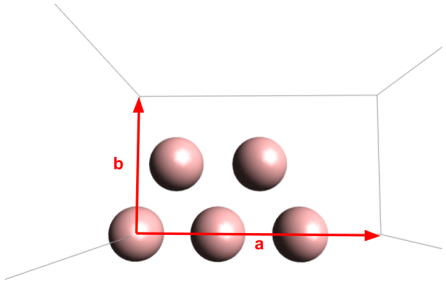

FIG. 1. Unit cell for β_{12}-borophene. Lattice constants a and b are indicated.

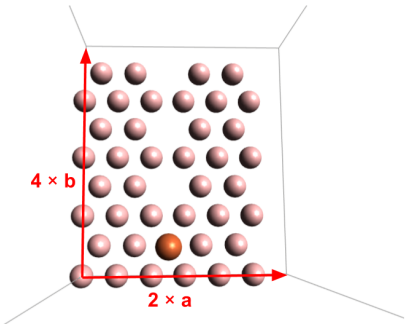

FIG. 2. The 4 × 2 supercell for doped β_{12}-borophene. The orange atom shows the position of the dopant on the surface. This supercell was used for Al-, Fe-, and Si-doped β_{12}-borophene catalysts.

ground-state energy can then be calculated for each value of a and b, with the lowest energy combination corresponding to the most energetically stable state. This process was initially performed on a course-grained scale, varying a from 4-6 Å and b from 2-4 Å, in steps of 0.5 Å. This was repeated on progressively finer grained scales until the third decimal place could be determined. A potential energy surface for the final run is shown in Figure 3, with the corresponding energy contour shown in Figure 4. In these Figures, a was varied from 5.05-5.08 Å in steps of 0.005 Å and b was varied from 2.92-2.94 in steps of 0.001 Å.

The purpose of using 0.005 Å steps for a is to speed up the calculations, since this requires five times less data points in total than using 0.001 Å for both lattice constants, and hence the calculation is five times faster. The third decimal place for a was determined by fitting polynomials to energy cross sections on the potential energy surface. For each polynomial, a value of b is fixed, and the polynomial is fitted to the energy values at each a. This results in seven data points for each polynomial, so sixth degree polynomials are used in order to maximised accuracy while maintaining uniqueness for the solutions. The lowest energy point among all polynomials can then be found, and the corresponding values of a and b are determined. The polynomial fits in Figure 5 resulted in values of $a = 5.066$ Å, and $b = 2.929$ Å. These values can be compared to those found by Peng et al in another first principles investigation of β_{12}-borophene, which reported $a = 5.07$ Å, and $b = 2.93$ Å [24]. These values are only reported to three significant figures, but nonetheless agree with the results presented here accounting for rounding.

Al, Fe, and Si atoms were placed 2 Å above the vacant areas in a 4 × 2 β_{12}-borophene supercell, as shown in Figure 2. This particular supercell was used so that the repeating two-dimensional surfaces will be identical to the surface used by Liu et al [3], which allows the reaction pathway diagrams obtained in this report to be directly compared to theirs. The adsorption energies for Al, Fe, and Si on β_{12}-borophene were found to be -4.07 eV, -8.26 eV, and -5.64 eV, respectively. These values were calculated using Equation 3. Lower (more negative) values indicate that the dopant is more energetically stable on the β_{12}-borophene surface, and hence less likely to detach during the reaction process. All three catalysts show reasonably strong adsorption, although Fe is clearly more stable than the other elements considered. This gives a good indication that these elements, and particularly Fe, will be resistant to certain types of catalytic poisoning, e.g.

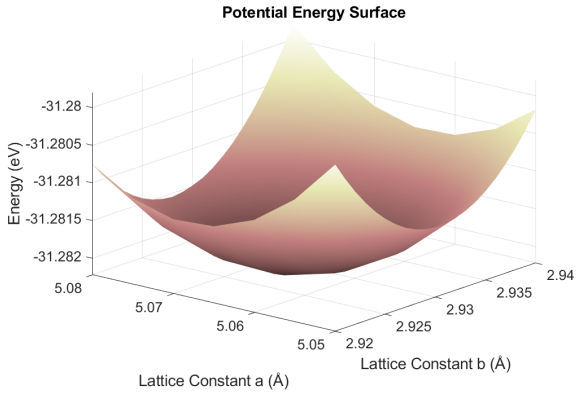

FIG. 3. Three-dimensional surface plot of the ground-state energy of the β_{12}-borophene lattice as a function of lattice constants a and b. The colouring of the surface has been interpolated to give a clearer visual indication of the shape.

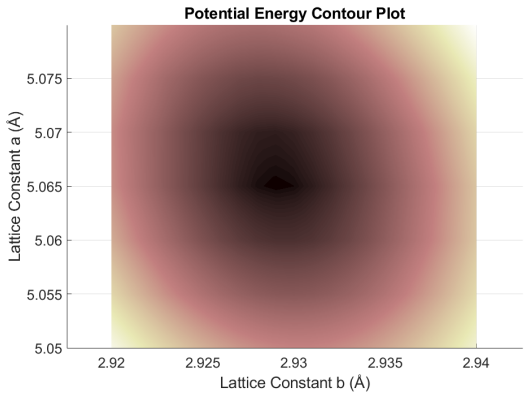

FIG. 4. 2D surface plot of the ground-state energy of the β_{12}-borophene lattice as a function of lattice constants a and b. The colouring of the surface has been interpolated to give a clearer visual indication of the shape.

reactive contaminants in the electrolytic solution will be less likely to replace the dopants if they bond strongly to the β_{12}-borophene surface.

When the atoms are doped onto the β_{12}-borophene surface, they cause the surface to deform. The distortions can be seen in Figure 6. The distortions are most prominent for the Fe dopant, which causes much of the β_{12}-borophene surface to bend towards it. This high degree of deformation is a characteristic property of two-dimensional materials, and contributes to the unique properties they display as electrocatalysts. This can be explored by looking at the way the deformations change between intermediate steps. Figure 7 shows the relaxed systems for Fe-doped β_{12}-borophene with two different reaction intermediates above the active site. The reaction progresses from O*CH_2,

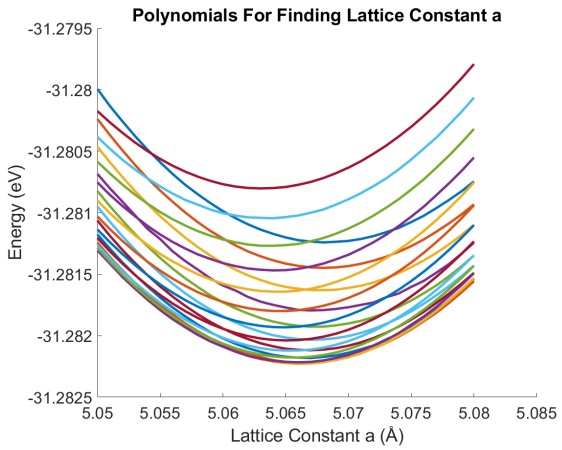

FIG. 5. Polynomials fitted to the energy cross sections of the potential energy surface in Figure 3. From these, the lattice constants are determined to be $a = 5.066$ Å, and $b = 2.929$ Å.

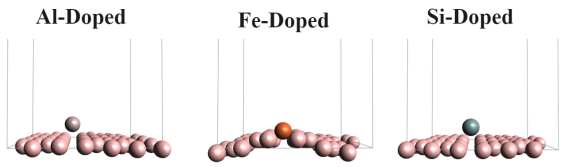

FIG. 6. Al, Fe, and Si on the β_{12}-borophene lattice. Distortions are very prominent for Fe, but are barely noticeable for both Al and Si.

shown in (a), to O*CH_3, shown in (b), via a single protonation step. The latter intermediate causes the surface distortions to relax, likely allowing the system to experience greater energy changes than if the catalyst were rigid and three-dimensional. This property doesn't necessarily correspond to desirable catalysts, but it does show that two-dimensional system exhibit exotic catalytic behaviour. Given that conventional catalysts are yet to produce adequate results for CO_2 reduction, exploring materials with exotic properties is a promising direction for this area of research.

Figure 8 shows the likely reaction pathways for electrochemical reduction of CO_2 into CH_4 and CH_3OH. Ideally, catalysts should show high selectivity for the production of CH_3OH, although CH_4 is also considered to be a viable fuel. Good catalysts should also show low selectivity for CO, which is a toxic gas and not particularly useful as a fuel. Considering as many reaction pathways as possible is crucial for systematically assessing the effectiveness of a catalyst; however, not all of the reaction pathways shown in Figure 8 are explored in this report. This is because not all

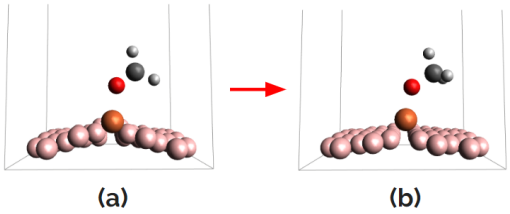

FIG. 7. A single protonation step for an intermediate on Fe-doped β_{12}-borophene. The transition is between (a) O*CH_2 and (b) O*CH_3

Dopant	PDS (eV)	U_{eq} (product)	η(V)
Al	0.940	-1.06 (CO)	0.798
Fe	0.152	0.169 (CH_4)	0.321
Si	0.835	-1.06 (CO)	0.729

TABLE II. Overpotentials, equilibrium potentials [3] and potential determining steps for each catalyst.

pathways are likely to contain the PDS, which is the relevant quantity for determining the overpotential for each catalyst. This approach was also taken by Liu et al [3] in their investigation of metal-doped β_{12}-borophene, so replicating this method here makes the results obtained in this report directly comparable to their work.

Catalytic performance is determined by placing (most of) the intermediate compounds shown in Figure 8 above the active dopant site, and letting the system relax so that its ground-state energy can be determined. The energies of each reaction step can then be determined using Equation 4, where the spectator molecules are found from the complete formation reactions shown in Table I. These energies are used to create reaction pathway diagrams, which for Fe-, Al-, and Si-doped β_{12}-borophene are shown in Figures 9, 10, and 11, respectively. The PDS for the primary reduction product is also indicated on each of these diagrams.

The primary reduction products for an electrocatalyst can be determined by looking at the value of the Gibbs free energy change at its PDS, ΔG_{PDS}. The product with the smallest ΔG_{PDS} will be the primary reduction product, and the selectivity of the catalyst will be proportional to the ratio of ΔG_{PDS} between the different products. For Fe, this means that CH_4 is highly selected for because of the very small $\Delta G_{PDS} = 0.152$ eV. For Al, the primary reduction product is CO with $\Delta G_{PDS} = 0.904$ eV, although this is closely followed by CH_4 with $\Delta G_{PDS} = 0.940$ eV. For Si, the primary reaction isn't as clear as the other elements because the potential determining step occurs along the shared path for CH_4 and CO. However, the primary reduction product will likely be CO, since disregarding the initial PDS, CO would have the smallest $\Delta G_{PDS} = 0.191$.

The PDS can be used to calculate the overpotential from Equation 5. The overpotentials for each catalyst are shown in Table II. Lower overpotentials correspond to lower voltages required to drive the electrolysis reaction. If the overpotential is higher than 2.21 V, which is the potential required for direct CO_2 reduction at the electrode [25], then the catalyst can be ruled out completely. The β_{12}-borophene with no dopant is a catalyst that can be ruled out in this way, as can be seen in the reaction pathway diagram in Figure 12. The PDS for every reaction product is 8.596 eV, which will correspond to an overpotential greater than 2.21 V for every reaction product. Hence, β_{12}-borophene by itself cannot be used as a catalyst for CO_2 reduction. This result was also found be Qin et al [26], where it was determined that β_{12}-borophene cannot form strong enough bonds with reaction intermediates to facilitate electrolysis. This result can be explored further by referring to Figure 13, where an OCHO molecule is shown adsorbed onto the β_{12}-borophene surface. Note that this molecule corresponds to the very large PDS in Figure 12, and that a B atom is drawn from the surface towards the OHCO molecule. Based on these results, it seems that deformation of the β_{12}-borophene surface becomes much more energetically feasible when a dopant is present.

The overpotential calculated for Fe-doped β_{12}-borophene, $\eta = 0.321$ V, is slightly lower than the value obtained by Liu et al, which found $\eta = 0.45$ V [3]. This difference in η can likely be explained by the more complicated theoretical method used in their report, which assumed a reaction temperature of 298.15 K and took into account the entropy changes at each reaction step when calculating the Gibbs free energy. This can be explored further by comparing the reaction pathway diagram for Fe-doped β_{12}-borophene from their report, shown in Figure 14, to the equivalent diagram presented in this report, in Figure 9. The shapes of the two graphs are clearly in strong agreement with each other, while the magnitude of the net energy changes do not agree so closely. While the overall value of η is calculated to be quite similar from either diagram, the differences are significant enough that the two diagrams do not agree on which step is the PDS. This demonstrates that entropy contributions can be quite significant, and should be included in electrochemical analysis wherever possible.

The value of η for Fe-doped β_{12}-borophene is

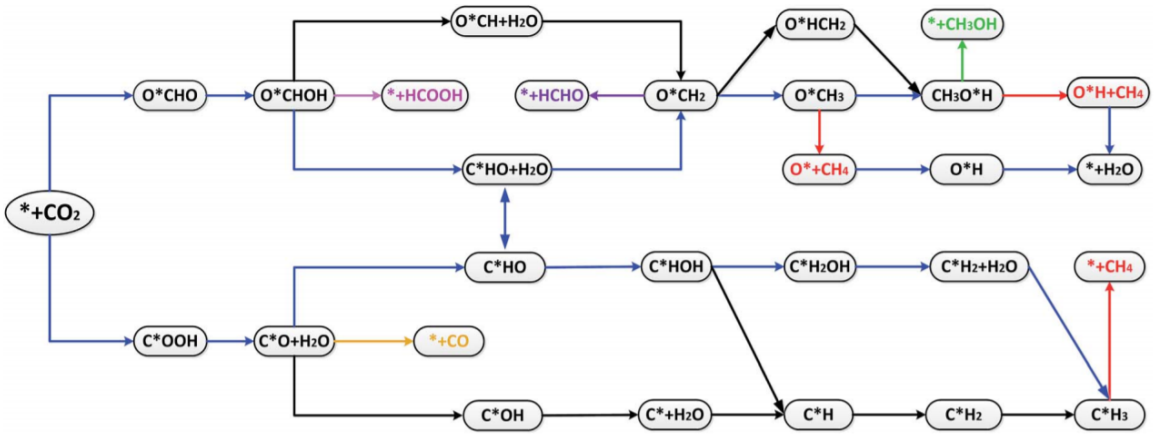

FIG. 8. Likely reaction pathways for CO_2 reduction [3]

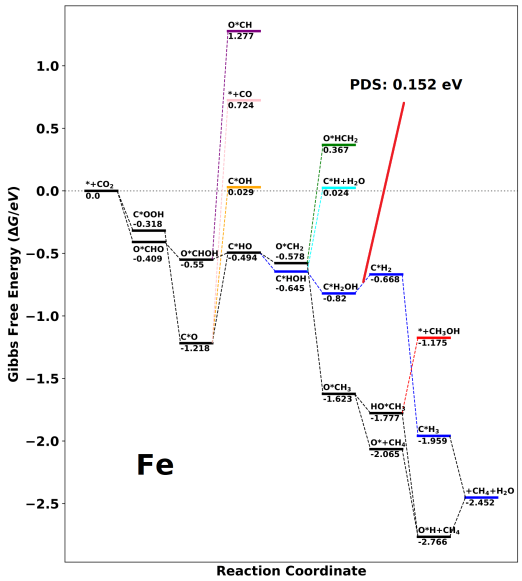

FIG. 9. Reaction pathways for CO_2 reduction on Fe-doped β_{12} borophene.

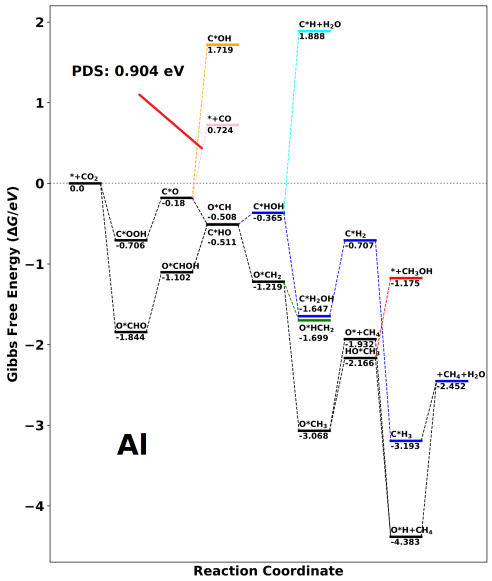

FIG. 10. Reaction pathways for CO_2 reduction on Al-doped β_{12} borophene.

found to be quite low, making it comparable or even superior to other well studied catalysts for producing CH_4, such as metallic Cu surfaces [27, 28]. Both Al and Si have relatively high overpotentials and largely produce CO, so neither of these newly explored catalysts are very promising by themselves. While Si-doped β_{12}-borophene was shown to be an ineffective catalyst by itself, it does show some desirable properties, e.g. the change in Gibbs free energy between methanol adsorbed onto the catalyst surface and methanol being released from the surface is extremely low. For the other catalysts studied here, this step where CH_3OH is released from the surface causes a large increase in Gibbs free energy. This is the step which limits the production of CH_3OH in Al and Fe. It's possible that well engineered combinations of various elements on a β_{12}-borophene surface could combine desirable energy steps from different catalysts to achieve feasible production of CH_3OH.

It should be noted that none of the reaction pathway diagrams in this report take into account the reaction barriers between intermediate reaction steps. Reaction barriers correspond to the energy

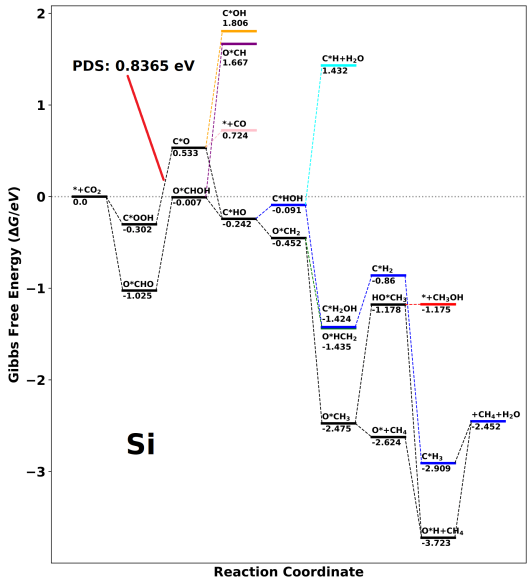

FIG. 11. Reaction pathways for CO_2 reduction on Si-doped β_{12} borophene.

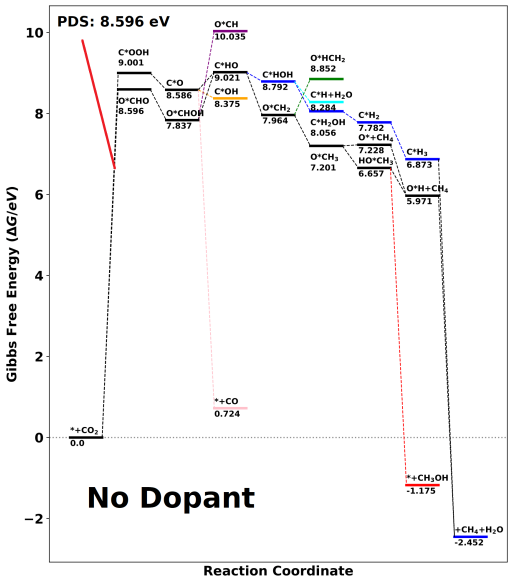

FIG. 12. Reaction pathways for CO_2 reduction on β_{12}-borophene.

required for molecules to geometrically transition as they react with the catalyst or other molecules. Determining these barriers is essential for rigorously calculating the overpotentials for a catalyst, as they may change the PDS of the reaction pathways. The reaction barriers can be calculated with DFT using the climbing image nudged elastic band method (CINEB) [29]. Currently, the lack of reaction barrier calculations is significant

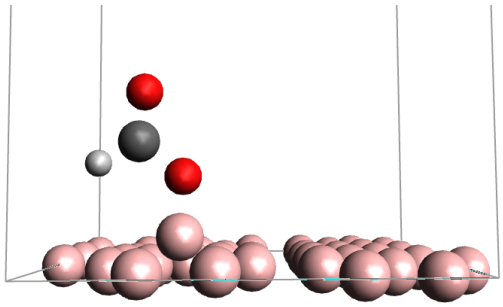

FIG. 13. OCHO adsorbed on the surface of β_{12}-borophene with no dopant.

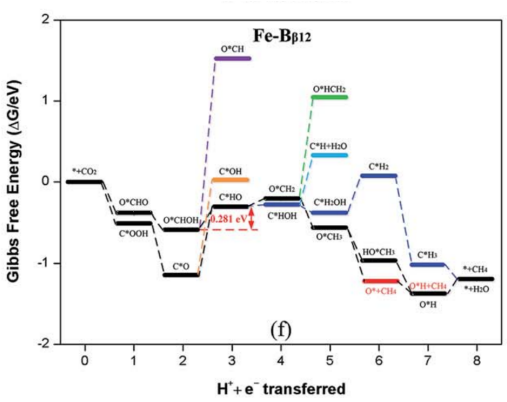

FIG. 14. Reaction pathways diagram for for CO_2 reaction pathways on Fe-doped β_{12}-borophene. This diagram is taken from another report [3], and assumes the reaction occurs at room temperature (298.15 K) for the purposes of taking into account the Gibbs free energy.

limitation on the confidence with which we can conclude the overpotentials for the considered catalysts.

SOFTWARE DESCRIPTION AND USE

The software provided alongside this report automates the process of creating reaction pathway graphs for CO_2 reduction, such as Figures 9, 10, 11, and 12. It has also been written is a way that makes it easy to adapt to other reactions of interest. Given VASP files containing potential catalysts, the software uses a Bash script to create nineteen further VASP jobs per catalyst. Each job contains a reaction intermediate placed 2 Å above the active site of the catalyst. Once these VASP jobs have been run, another Bash script can be used to automatically plot the reaction pathway diagrams. The software is designed to run with almost no configuration needed - the settings for the generated VASP

jobs are simply extracted from those already being used for the catalysts.

Each VASP job consists of four files which specify the parameters of the system to be simulated: the POSCAR file specifies the positions of the atoms, the POTCAR file specifies the pseudo-potentials to be used for each atom, the KPOINTS file specifies the k-sampling method and the number of k-points used in each direction, and the INCAR file specifies other miscellaneous settings. Additionally, a run file is needed to start the VASP job itself, which is set by default to be a Portable Batch System (PBS) file, as used by the High Performance Computing Cluster (HPCC) at The University of Sydney. After a VASP job has been run, additional files are created which specify the results. Notably, the CONTCAR file contains the final positions of the atoms.

To use the software, VASP jobs containing catalysts are placed in a directory called "Surfaces". The file "CreateJobs.sh" is then run within a UNIX environment. Nineteen new VASP jobs will then be created for each catalyst. For each of these new jobs, the KPOINTS file is directly copied from the catalyst. The PBS run file is also copied over, but the name of the job is changed to follow the format of "catalyst_intermediate". A suitable POTCAR file is made by appending combinations of C, O and H POTCAR files to the POTCAR file used by the catalyst. By default, PBE [10] pseudo-potentials are used, but these can easily be replaced by swapping out the POTCAR files contained in the "IndividualPOTCARs" directory. An INCAR file is then made by copying over the catalyst's INCAR file, and if magnetic moments have been specified in this file, then the magnetic moments of the intermediates are added (for CO_2 reduction, all of these magnetic moments are zero). Creating the POSCAR file is more difficult than the previous steps. The lattice constants, scaling factor, and position of the last atom are read from the catalyst's CONTCAR file. The lattice constants and scaling factor are used to adjust the fractional coordinates of molecules in the intermediate's unit cell to those in the catalyst's cell, ensuring that the physical distance between molecules is preserved. This coordinate conversion in any given direction can be expressed as

$$F_2 = \frac{L_1 S_1}{L_2 S_2} F_1$$

Where F indicates fractional coordinates, L indicates lattice constants, S indicates scaling factor, and the subscripts 1 and 2 indicate the intermediate cell and catalyst cell, respectively. The converted intermediate coordinates are then translated so that the intermediate sits 2 Å above last atom specified in the CONTCAR file, which is assumed to be the active site of the catalyst.

The resulting VASP jobs are organised by catalyst name, contained in the "jobs" directory. Also in this directory will be a "runAllJobs" script for running every generated job, which by default is written in C Shell for use in the HPCC. An equivalent script written in Bash has been included in the "CreateJobs.sh" file, and needs to be uncommented if Bash is the preferred shell.

Once the jobs have finished running, the reaction pathways can be plotted by running "PlotEnergies.sh". This script makes use of and extends the "EnergyLeveller" python module [30] to plot the reaction pathways based on the ground-state energies calculated by VASP. The links between intermediates, colour schemes, and balanced equations are specified in the "PlotEnergies.sh" file. The resulting graphs will be placed in the "plots" directory in the form of PDF files, along with a corresponding ".inp" file which can be used to make adjustments to the graphs. A few extra features have been added manually to the EnergyLeveller Python module, which extend it's ability to format the resulting graphs. In particular, if any of the labels on the graph are overlapping, then the "Move Up = true" or "Move Down = true" tag can be added to the relevant states in the ".inp" file, followed by running the "EnergyLeveller.py" script. Other features that have been added include the ability to configure the diagram widths, and options to adjust the size of fonts on axis labels.

CONCLUSION

In this report, Al-, Fe-, and Si-doped β_{12}-borophene are investigated as potential catalysts for CO_2 reduction using DFT. The lattice constants for β_{12}-borophene have also been calculated, with values of $a = 5.066$, $b = 2.929$, which are in strong agreement with those reported by Peng et al [24]. Furthermore, these values are reported to an additional significant figure of accuracy. All three dopants considered showed reasonably strong adsorption onto the β_{12}-borophene surface, although Fe had significantly stronger adsorption than the other elements considered at -8.26 eV. Fe-doped β_{12}-borophene is also shown to be highly selective for the production of methane in agreement with results found by Liu et al [3]. Al- and Si-doped β_{12}-borophene are shown to produce mostly CO, and do so with with a relatively high overpotential. This shows that Al- and Si-doped β_{12}-borophene are not effective catalysts for CO_2 reduction, while Fe-doped β_{12}-borophene is effective if the desired product methane. None of the

catalysts considered showed selectivity for methanol. The software for automating the investigation of these catalysts has been shown to work effectively based on the replication of the reaction pathway diagram for Fe-doped β_{12}-borophene. Considering the relatively poor performance of the newly considered catalysts in this report (Al- and Si-doped β_{12}-borophene), the software will likely prove to be the most useful result presented here by dramatically reducing the number of man-hours needed to investigate potential catalysts in the future. This will also reducing the chances of human error in generating these results.

A promising avenue of future work would be to further the automation of catalyst exploration to the point where the entire process, from catalyst generation to calculation of the overpotential, is automated. If this process was sufficiently optimised, then it would allow for many different catalyst designs to be exhaustively tested, and the potential for finding catalysts with smaller overpotentials would greatly increase. This would additionally allow for the creation of large datasets that could be used to train machine learning algorithms. These may be able to find patterns and design new catalysts that reduce the overpotentials even further. Another interesting area that needs further investigation is the impact of temperature on the overpotentials for a given catalyst. As demonstrated by comparing Figures 9 and 14, the contribution of entropy, and hence temperature at which the reactions occur, can change the PDS and the corresponding overpotential for a catalyst. Optimising the temperature at which electrolysis is performed for other well known catalysts could potentially yield smaller overpotentials than have previously been discovered.

Finally, the theoretical methods used in this report require a great deal of further research. As previously mentioned, the methods should be expanded to include reaction barriers and entropy calculations, among other physical nuances present in the real-life reactions. Additionally, The validity of these methods should also be explored by applying them to catalysts for which the catalytic performance is experimentally known, and for catalysts that produce a variety of different reaction products. Cu-cuprous oxide is an example of such a catalyst, which has low, experimentally determined overpotentials for electrolytic reduction of CO_2 into ethanol and acetic acid [31].

[1] S. Davis, K. Caldeira, and H. D. Matthews, Future CO_2 emissions and climate change from existing energy infrastructure, Science (New York, N.Y.) **329**, 1330 (2010).

[2] S. O. Amrouche], D. Rekioua, T. Rekioua, and S. Bacha, Overview of energy storage in renewable energy systems, International Journal of Hydrogen Energy **41**, 20914 (2016).

[3] J.-H. Liu, L.-M. Yang, and E. Ganz, Efficient electrocatalytic reduction of carbon dioxide by metal-doped 12 -borophene monolayers, RSC Advances **9**, 27710 (2019).

[4] Nist chemistry webbook, Available at `https://webbook.nist.gov/`.

[5] G. Myhre, D. Shindell, F.-M. Bréon, W. Collins, J. Fuglestvedt, J. Huang, D. Koch, J.-F. Lamarque, D. Lee, B. Mendoza, T. Nakajima, A. Robock, G. Stephens, T. Takemura, and H. Zhang, Anthropogenic and natural radiative forcing, in *Climate Change 2013: The Physical Science Basis. Contribution of Working Group I to the Fifth Assessment Report of the Intergovernmental Panel on Climate Change*, edited by T. F. Stocker, D. Qin, G.-K. Plattner, M. Tignor, S. K. Allen, J. Doschung, A. Nauels, Y. Xia, V. Bex, and P. M. Midgley (Cambridge University Press, Cambridge, UK, 2013) pp. 659–740.

[6] J. W. Morgan and E. Anders, Chemical composition of earth, venus, and mercury, Proceedings of the National Academy of Sciences **77**, 6973 (1980), https://www.pnas.org/content/77/12/6973.full.pdf.

[7] D. S. Sholl and J. A. Steckel, *Density Functional Theory* (John Wiley Sons, Ltd, 2009) Chap. 1-2, pp. i–xii.

[8] B. Miehlich, A. Savin, H. Stoll, and H. Preuss, Results obtained with the correlation energy density functionals of Becke and Lee, Yang and Parr, Chemical Physics Letters **157**, 200 (1989).

[9] D. C. Langreth and M. J. Mehl, Beyond the local-density approximation in calculations of ground-state electronic properties, Phys. Rev. B **28**, 1809 (1983).

[10] J. P. Perdew, K. Burke, and M. Ernzerhof, Generalized gradient approximation made simple [Phys. Rev. Lett. 77, 3865 (1996)], Phys. Rev. Lett. **78**, 1396 (1997).

[11] G. Kresse and J. Hafner, *Ab initio* molecular dynamics for liquid metals, Phys. Rev. B **47**, 558 (1993).

[12] G. Kresse and J. Hafner, *Ab initio* molecular-dynamics simulation of the liquid-metal–amorphous-semiconductor transition in germanium, Phys. Rev. B **49**, 14251 (1994).

[13] G. Kresse and J. Furthmüller, Efficiency of *ab-initio* total energy calculations for metals and semiconductors using a plane-wave basis set, Computational Materials Science **6**, 15 (1996).

[14] G. Kresse and J. Furthmüller, Efficient iterative schemes for *Ab initio* total-energy calculations using a plane-wave basis set, Physical Review B **54**,

11169 (1996).
[15] S. Grimme, J. Antony, S. Ehrlich, and H. Krieg, A consistent and accurate *ab initio* parametrization of density functional dispersion correction (dft-d) for the 94 elements H-Pu, The Journal of Chemical Physics **132**, 154104 (2010), https://doi.org/10.1063/1.3382344.
[16] S. Grimme, S. Ehrlich, and L. Goerigk, Effect of the damping function in dispersion corrected density functional theory, Journal of Computational Chemistry **32**, 1456 (2011).
[17] Vasp documetiaton on setting magnetic moments, Available at `https://www.vasp.at/wiki/index.php/MAGMOM`.
[18] M. D. Hanwell, D. E. Curtis, D. C. Lonie, T. Vandermeersch, E. Zurek, and G. R. Hutchison, Avogadro: an advanced semantic chemical editor, visualization, and analysis platform, Journal of cheminformatics **4**, 17 (2012).
[19] A. K. Rappe, C. J. Casewit, K. S. Colwell, W. A. Goddard, and W. M. Skiff, UFF: a full periodic table force field for molecular mechanics and molecular dynamics simulations, Journal of the American Chemical Society **114**, 10024 (1992).
[20] J. Lee, *Computational Materials Science: An Introduction* (Taylor & Francis, 2011).
[21] K. Reuter and M. Scheffler, Composition, structure, and stability of $RuO_2(110)$ as a function of oxygen pressure, Phys. Rev. B **65**, 035406 (2001).
[22] M. Koper, Analysis of electrocatalytic reaction schemes: Distinction between rate-determining and potential-determining steps, Journal of Solid State Electrochemistry **17** (2012).
[23] F. Gossenberger, T. Roman, and A. Gross, Hydrogen and halide co-adsorption on Pt(111) in an electrochemical environment: a computational perspective, Electrochimica Acta **216**, 152 (2016).
[24] B. Peng, H. Zhang, H. Shao, Z. Ning, Y. Xu, H. Lu, D. Zhang, and H. Zhu, Stability and strength of atomically thin borophene from first principles calculations, Materials Research Letters **5** (2016).
[25] Y. Hori, Electrochemical co_2 reduction on metal electrodes, in *Modern Aspects of Electrochemistry*, edited by C. G. Vayenas, R. E. White, and M. E. Gamboa-Aldeco (Springer New York, New York, NY, 2008).
[26] Q. Sun, G. Qin, Q. Cui, and A. Du, Borophene: A metal-free and metallic electrocatalyst for efficient converting co2 into ch4, ChemCatChem **12** (2019).
[27] A. Peterson, F. Abild-Pedersen, F. Studt, J. Rossmeisl, and J. Nørskov, How copper catalyzes the electroreduction of carbon dioxide into hydrocarbon fuels, Energy Environmental Science **3**, 1311 (2010).
[28] K. P. Kuhl, E. R. Cave, D. N. Abram, and T. F. Jaramillo, New insights into the electrochemical reduction of carbon dioxide on metallic copper surfaces, Energy Environ. Sci. **5**, 7050 (2012).
[29] B. Uberuaga and H. Jonsson, A climbing image nudged elastic band method for finding saddle points and minimum energy paths, J. Chem. Phys. **113**, 9901 (2000).
[30] J. Furness, Energyleveller, Available at `https://github.com/BackgroundNose/EnergyLeveller`.
[31] Q. Zhu, X. Sun, D. Yang, J. Ma, X. Kang, L. Zheng, J. Zhang, Z. Wu, and B. Han, Carbon dioxide electroreduction to C_2 products over copper-cuprous oxide derived from electrosynthesized copper complex, Nature Communications **10**, 3851 (2019).

Appendix A: Code for CreateJobs.sh

```
#!/bin/bash
#ONLY WORKS WITH FRACTIONAL COORDINATES
#ONLY WORKS WITH RECTANGULAR LATTICE VECTORS
#Set the name of the molecule
#SET RUN FILE EXTENSION USED ON MACHINE - Default set to .csh for USYD physics cluster
EXT="csh"
mkdir jobs
MAGMOM=-1
for ATOM in $(ls Surfaces)
do
    mkdir jobs/${ATOM}
    for MOL in $(ls Molecules)
    do
        #Create the right POTCAR file
        mkdir jobs/${ATOM}/${MOL}
        cat Surfaces/${ATOM}/POTCAR >> jobs/${ATOM}/${MOL}/POTCAR
        if [[ "$MOL" == *"C"* ]]
        then
            cat IndividualPOTCARs/C-POTCAR >> jobs/${ATOM}/${MOL}/POTCAR
        fi
        if [[ "$MOL" == *"O"* ]]
        then
            cat IndividualPOTCARs/O-POTCAR >> jobs/${ATOM}/${MOL}/POTCAR
        fi
        if [[ "$MOL" == *"H"* ]]
        then
            cat IndividualPOTCARs/H-POTCAR >> jobs/${ATOM}/${MOL}/POTCAR
        fi

        #Use same KPOINTS as in surface
        cp Surfaces/${ATOM}/KPOINTS jobs/${ATOM}/${MOL}/KPOINTS

        #Create INCAR File
        MOLLENGTH=`wc -l Molecules/${MOL} | awk '{print $1}'`
        cat Surfaces/${ATOM}/INCAR  | sed 's/!.*//g' | sed 's/#.*//g' | sed '/^[[:space:]]*$/d' \
        | sed 's/MAGMOM.*/& '"${MOLLENGTH}*0.0/" > jobs/${ATOM}/${MOL}/INCAR

        #Create run.csh file
        cat Surfaces/${ATOM}/run.${EXT} | sed 's/-N .*/'"-N ${ATOM}_${MOL}/" > jobs/${ATOM}/${MOL}/run.${EXT}

        #Create POSCAR
        #Count number of each atom in files
        CS=0
        OS=0
        HS=0
        while read line || [ -n "$line" ]
        do
            LETTER=`echo $line | awk '{print $1}'`
            if [[ $LETTER == C ]]
            then
                let "CS+=1"
            fi
            if [[ $LETTER == O ]]
            then
                let "OS+=1"
            fi
            if [[ $LETTER == H ]]
            then
                let "HS+=1"
            fi
        done < Molecules/$MOL
        NUMS=""
        if [[ $CS > 0 ]]
        then
            NUMS="$NUMS $CS"
        fi
        if [[ $OS > 0 ]]
        then
            NUMS="$NUMS $OS"
        fi
        if [[ $HS > 0 ]]
        then
            NUMS="$NUMS $HS"
        fi
        #Insert first part of POSCAR
        #This takes the CONTCAR and removes the last section - based on the empty line that separates
        #The molecule positions from
        cat Surfaces/${ATOM}/CONTCAR | sed '/^ *$/Q' | sed '6d' | sed '6s/.*/&'"${NUMS}/" > jobs/${ATOM}/${MOL}/POSCAR
        lastChar=`tail -c1 jobs/${ATOM}/${MOL}/POSCAR`

        #Get cell shape from surface
        Scale=`sed -n 2p Surfaces/$ATOM/CONTCAR | awk '{print $1}'`
        XC=`sed -n 3p Surfaces/$ATOM/CONTCAR | awk '{print $1}'`
        YC=`sed -n 4p Surfaces/$ATOM/CONTCAR | awk '{print $2}'`
        ZC=`sed -n 5p Surfaces/$ATOM/CONTCAR | awk '{print $3}'`
```

```
#Get the last molecule coordinates
        X=‘tail -1 jobs/${ATOM}/${MOL}/POSCAR | awk ’{print $1}’‘
        Y=‘tail -1 jobs/${ATOM}/${MOL}/POSCAR | awk ’{print $2}’‘
        Z=‘tail -1 jobs/${ATOM}/${MOL}/POSCAR | awk ’{print $3}’‘

        #Please note that the constant values of 10.16, 11.76, and 15 are the x, y, z lattice constants
        #for the intermediate molecules. If another chemical reaction scheme is to be defined,
        #These can be changed to match whichever lattice constants are used.
        #This code converts fractional coordinates of intermediates and places them on top of surface (last atom)
        while read line || [ -n "$line" ]
        do
            echo $line | awk -v X=$X -v Y=$Y -v Z=$Z -v XC=$XC -v YC=$YC -v ZC=$ZC -v Scale=$Scale \
            ’{printf "  %1.5f %1.5f %1.5f\n", ($2*(10.16/(XC*Scale)))+X, ($3*(11.76/(YC*Scale)))+Y,\
             ($4*(15/(ZC*Scale)))+Z+(2/(ZC*Scale))}’ >> jobs/${ATOM}/${MOL}/POSCAR
        done < Molecules/$MOL
    done
done
#Create a run file with csh syntax. This can easily be adjusted for other shell types.
cat > jobs/runAllJobs.csh <<-EOF
#!/bin/csh
module load PBS
foreach d (\‘ls -d */\‘)
    cd \$d
    foreach e (\‘ls -d */\‘)
        cd "\$e"
        qsub run.csh
        cd ..
    end
    cd ..
end
EOF
#This is a run file for bash that would work equally well, still assuming PBS is used.
# cat > jobs/runAllJobs.sh <<-EOF
# #!/bin/sh
# module load PBS
# for d \$(ls -d */)
#     cd "\$d"
#     for e \$(ls -d */)
#         cd "\$e"
#         qsub run.sh
#         cd ..
#     end
#     cd ..
# end
# EOF
```

Appendix B: Code for PlotEnergies.sh

```
#!/bin/bash
#This program uses the Energy-Leveler python script to plot energy level diagrams for all of the created jobs.
#IN EVENT OF CONFLICT:
#USE MOVE UP = TRUE AND MOVE DOWN = TRUE
#Helper function to extract the ground-state energy from an OSZICAR file given as input
getGibbs() {
    E=$1
    E=$(echo $E | grep -o 'E0=.*d')
    E=$(echo $E | sed 's/E0= //g')
    E=$(echo $E | sed 's/\s*d//g')
    E=$(echo $E | sed "s/E+/*10^/")
    E=$(echo $E | bc)
    echo $E
}
#Energies of lone molecules
for MOL in $(ls LoneMolecules)
do
    declare "LONE_${MOL}_ENERGY"=$(getGibbs "`tail -1 LoneMolecules/${MOL}/OSZICAR`")
done
#Energies of atoms on surface
for SURFACE in $(ls Surfaces)
do
    SURFACE_ENERGY=$(getGibbs "`tail -1 Surfaces/${SURFACE}/OSZICAR`")
    BASE_ENERGY=$(echo "$SURFACE_ENERGY + $LONE_CO2_ENERGY + (4 * $LONE_H2_ENERGY)" | bc)

    #Energies of surfaces
    for MOL in $(ls Molecules)
    do
        declare "${MOL}_ENERGY"=$(getGibbs "`tail -1 jobs/${SURFACE}Sheet/${MOL}/OSZICAR`")
    done
    cat > EnergyLeveller-master/${SURFACE}_Energy_Plot.inp <<EOF
output-file     = ${SURFACE}_Energy_Plot.pdf
width           = 10
height          = 10
energy-units    = Gibbs Free Energy (\$\Delta G/eV\$)
font size       = 10
#   start at zero
############################################################################## COLUMN 1
{
    name        = CO2
    text-colour = black
    label       = *+CO\$_2\$
    energy      = 0.00
    labelColour = black
    linksto     = OCHO:black, COOH:black
    column      = 1
}
############################################################################## COLUMN 2
{
    name        = OCHO
    text-colour = black
    label       = O*CHO
    energy      = $(printf %.3f $(echo "${OCHO_ENERGY} - ${BASE_ENERGY} + (3.5 * ${LONE_H2_ENERGY})"| bc))
    labelColour = black
    linksto     = OCHOH:black
    column      = 2
}

{
    name        = COOH
    text-colour = black
    label       = C*OOH
    energy      = $(printf %.3f $(echo "${COOH_ENERGY} - ${BASE_ENERGY} + (3.5 * ${LONE_H2_ENERGY})" | bc))
    labelColour = black
    linksto     = CO:black
    column      = 2
}
############################################################################## COLUMN 3
{
    name        = CO
    text-colour = black
    label       = C*O
    energy      = $(printf %.3f $(echo "${CO_ENERGY} - ${BASE_ENERGY} ${LONE_H2O_ENERGY} + (3 * ${LONE_H2_ENERGY})"| bc))
    labelColour = black
    linksto     = CHO:black, COH:orange, +CO:pink
    column      = 3
}

{
    name        = OCHOH
    text-colour = black
    label       = O*CHOH
    energy      = $(printf %.3f $(echo "${OCHOH_ENERGY} - ${BASE_ENERGY} + (3 * ${LONE_H2_ENERGY})"| bc))
    labelColour = black
    linksto       = OCH:purple, CHO:black
    column      = 3
}
```

```
############################################################################## COLUMN 4
{
    name        = COH
    text-colour = orange
    label       = C*OH
    energy      = $(printf %.3f $(echo "${COH_ENERGY} - ${BASE_ENERGY} + ${LONE_H2O_ENERGY} + (2.5 * ${LONE_H2_ENERGY})"| bc))
    labelColour = black
    column      = 4
}

{
    name        = OCH
    text-colour = purple
    label       = O*CH
    energy      = $(printf %.3f $(echo "${OCH_ENERGY} - ${BASE_ENERGY} + ${LONE_H2O_ENERGY} + (2.5 * ${LONE_H2_ENERGY})" | bc))
    labelColour = black
    column      = 4
}

{
    name        = +CO
    text-colour = pink
    label       = *+CO
    energy      = $(printf %.3f $(echo "${SURFACE_ENERGY} + ${LONE_CO_ENERGY} - ${BASE_ENERGY} + ${LONE_H2O_ENERGY}\
    + (3 * ${LONE_H2_ENERGY})" | bc))
    labelColour = black
    column      = 4
}

{
    name        = CHO
    text-colour = black
    label       = C*HO
    energy      = $(printf %.3f $(echo "${CHO_ENERGY} - ${BASE_ENERGY} + ${LONE_H2O_ENERGY} + (2.5 * ${LONE_H2_ENERGY})" | bc))
    labelColour = black
    linksto       = CHOH:blue, OCH2:black
    column      = 4
}
############################################################################## COLUMN 5
{
    name        = CHOH
    text-colour = blue
    label       = C*HOH
    energy      = $(printf %.3f $(echo "${CHOH_ENERGY} - ${BASE_ENERGY} + ${LONE_H2O_ENERGY} + (2 * ${LONE_H2_ENERGY})" | bc))
    labelColour = black
    linksto       = CH2OH:blue, CH+H2O:cyan
    column      = 5
}

{
    name        = OCH2
    text-colour = black
    label       = O*CH\$_2\$
    energy      = $(printf %.3f $(echo "${OCH2_ENERGY} - ${BASE_ENERGY} + ${LONE_H2O_ENERGY} + (2 * ${LONE_H2_ENERGY})" | bc))
    labelColour = black
    linksto       = OCH3:black, OHCH2:green
    column      = 5
}
############################################################################## COLUMN 6
{
    name        = OHCH2
    text-colour = green
    label       = O*HCH\$_2\$
    energy      = $(printf %.3f $(echo "${OHCH2_ENERGY} - ${BASE_ENERGY} + ${LONE_H2O_ENERGY} + (1.5 * ${LONE_H2_ENERGY})" | bc))
    labelColour = black
    column      = 6
}

{
    name        = CH+H2O
    text-colour = cyan
    label       = C*H+H\$_2\$O
    energy      = $(printf %.3f $(echo "${CH_ENERGY} + ${LONE_H2O_ENERGY} - ${BASE_ENERGY}\
    + ${LONE_H2O_ENERGY} + (1.5 * ${LONE_H2_ENERGY})" | bc))
    labelColour = black
    column      = 6
}

{
    name        = CH2OH
    text-colour = blue
    label       = C*H\$_2\$OH
    energy      = $(printf %.3f $(echo "${CH2OH_ENERGY} - ${BASE_ENERGY} + ${LONE_H2O_ENERGY} + (1.5 * ${LONE_H2_ENERGY})" | bc))
    labelColour = black
    linksto       = CH2:blue
    column      = 6
}
```

```
{
    name        = OCH3
    text-colour = black
    label       = O*CH\$_3\$
    energy      = $(printf %.3f $(echo "${OCH3_ENERGY} - ${BASE_ENERGY} + ${LONE_H2O_ENERGY} + (1.5 * ${LONE_H2_ENERGY})" | bc))
    labelColour = black
    linksto        = O+CH4:black, HOCH3:black
    column      = 6
}
############################################################################## COLUMN 7
{
    name        = CH2
    text-colour = blue
    label       = C*H\$_2\$
    energy      = $(printf %.3f $(echo "${CH2_ENERGY} - ${BASE_ENERGY} + (2 * ${LONE_H2O_ENERGY}) + ${LONE_H2_ENERGY}" | bc))
    labelColour = black
    linksto        = CH3:blue
    column      = 7
}

{
    name        = O+CH4
    text-colour = black
    label       = O*+CH\$_4\$
    energy      = $(printf %.3f $(echo "${O_ENERGY} + ${LONE_CH4_ENERGY} - ${BASE_ENERGY}\
    + ${LONE_H2O_ENERGY} + ${LONE_H2_ENERGY}" | bc))
    labelColour = black
    linksto        = OH+CH4:black
    column      = 7
}

{
    name        = HOCH3
    text-colour = black
    label       = HO*CH\$_3\$
    energy      = $(printf %.3f $(echo "${HOCH3_ENERGY} - ${BASE_ENERGY} + ${LONE_H2O_ENERGY} + ${LONE_H2_ENERGY}" | bc))
    labelColour = black
    linksto        = OH+CH4:black, +CH3OH:red
    column      = 7
}
############################################################################## COLUMN 8
{
    name        = CH3
    text-colour = blue
    label       = C*H\$_3\$
    energy      = $(printf %.3f $(echo "${CH3_ENERGY} - ${BASE_ENERGY} + (2 * ${LONE_H2O_ENERGY}) + (0.5 * ${LONE_H2_ENERGY})" | bc))
    labelColour = black
    linksto        = +CH4+H2O
    column      = 8
}

{
    name        = +CH3OH
    text-colour = red
    label       = +CH\$_3\$OH
    energy      = $(printf %.3f $(echo "${SURFACE_ENERGY} + ${LONE_CH3OH_ENERGY} - ${BASE_ENERGY}\
    + ${LONE_H2O_ENERGY} + ${LONE_H2_ENERGY}" | bc))
    labelColour = black
    column      = 8
}

{
    name        = OH+CH4
    text-colour = black
    label       = O*H+CH\$_4\$
    energy      = $(printf %.3f $(echo "${OH_ENERGY} + ${LONE_CH4_ENERGY} - ${BASE_ENERGY}\
    + ${LONE_H2O_ENERGY} + (0.5 * ${LONE_H2_ENERGY})" | bc))
    labelColour = black
    linksto        = +CH4+H2O:black
    column      = 8
}
############################################################################## COLUMN 9
{
    name        = +CH4+H2O
    text-colour = blue
    label       = +CH\$_4\$+H\$_2\$O
    energy      = $(printf %.3f $(echo "${SURFACE_ENERGY} + ${LONE_CH4_ENERGY} + ${LONE_H2O_ENERGY}\
    - ${BASE_ENERGY} + ${LONE_H2O_ENERGY}" | bc))
    labelColour = black
    column      = 9
}
EOF
    #Run the energy level plotter
    python3 EnergyLeveller-master/EnergyLeveller.py EnergyLeveller-master/${SURFACE}_Energy_Plot.inp
    mv "${SURFACE}_Energy_Plot.pdf" ./plots #2>/dev/null
    mv "EnergyLeveller-master/${SURFACE}_Energy_Plot.inp" ./plots #2>/dev/null
done
```